actuators

MDPI

Article

Soft Controllable Carbon Fibre-based Piezoresistive Self-Sensing Actuators

Min Pan [1,*], Chenggang Yuan [1], Hastha Anpalagan [1], Andrew Plummer [1], Jun Zou [2], Junhui Zhang [2] and Chris Bowen [1,*]

[1] Department of Mechanical Engineering, University of Bath, Bath BA2 7AY, UK; cy466@bath.ac.uk (C.Y.); hca30@bath.ac.uk (H.A.); arp23@bath.ac.uk (A.P.)

[2] Key Laboratory of Fluid Power and Mechatronic Systems, Zhejiang University, Hangzhou 310027, China; junzou@zju.edu.cn (J.Z.); benzjh@zju.edu.cn (J.Z.)

* Correspondence: m.pan@bath.ac.uk (M.P.); msscrb@bath.ac.uk (C.B.)

Received: 18 July 2020; Accepted: 29 August 2020; Published: 30 August 2020

Abstract: Soft robots and devices exploit deformable materials that are capable of changes in shape to allow conformable physical contact for controlled manipulation. While the use of embedded sensors in soft actuation systems is gaining increasing interest, there are limited examples where the body of the actuator or robot is able to act as the sensing element. In addition, the conventional feedforward control method is widely used for the design of a controller, resulting in imprecise position control from a sensory input. In this work, we fabricate a soft self-sensing finger actuator using flexible carbon fibre-based piezoresistive composites to achieve an inherent sensing functionality and design a dual-closed-loop control system for precise actuator position control. The resistance change of the actuator body was used to monitor deformation and fed back to the motion controller. The experimental and simulated results demonstrated the effectiveness, robustness and good controllability of the soft finger actuator. Our work explores the emerging influence of inherently piezoresistive soft actuators to address the challenges of self-sensing, actuation and control, which can benefit the design of next-generation soft robots.

Keywords: soft actuators; flexible piezoresistive sensor; self-sensing actuator; controllable soft robots

1. Introduction

Soft robots are defined as "soft systems" that use materials with elastic moduli comparable to soft biological materials (10^4–10^9 Pa) and are capable of autonomous behaviour. Such robots possess many attributes that are difficult to achieve using conventional rigid robots. For example, they are often more resilient and safer than their rigid counterparts during interaction with humans and are able to adapt to the natural environment due to high compliance of their soft bodies. They are also generally cost-effective and easy to manufacture compared to rigid systems. The applications of soft actuators and robots include biomedical devices [1], surgical instruments [2], rehabilitation systems [3], assistive devices [4,5], and robots for exploration and rescue [6].

Significant progress in the development and advancement of soft actuators and robots has been achieved in the last decade to achieve mechanical flexibility, adaptability, ease of manufacture and low-cost processing. To achieve their full potential, the key underpinning technologies of material science, sensing, and actuation must be effectively integrated and operate cooperatively. Therefore, technologies that couple both sensing and actuation are critical to accelerating the design and implementation of future soft robots [7,8]. Researchers have created new materials for soft actuation, including shape-memory materials, polyelectrolyte gels, electro-active polymers, ionic liquids and polymers and carbon nanotubes [7]. New sensing technologies and mechanisms have also been developed for monitoring the deformation of

soft robots, including piezoresistance (a change in resistance with stress) [8], piezocapacitive (a change in capacitance with stress) [9], piezoelectric (voltage or charge generation with stress) [10], thermal sensors [11] and multifunctional electronic skins (e-skins) [12].

Stretchable capacitive sensors have been recently used for soft robotics and wearable devices. The sensor normally consists of a thin dielectric layer sandwiched between a pair of conductors, providing an effective approach to measure strain, force, bending and shear of soft actuators and devices. The capacitance variation relies on the change in dielectric thickness and effective overlapping electrode surface area. Compared to resistive sensors, this method can overcome hysteresis caused by changes in the electrical resistivity of conductors, demonstrating high sensitivity, repeatability and temperature stability. Cataldi et al. fabricated highly sensitive capacitors by spraying coating nitrile rubber gloves with conductive rubbery slurries containing carbon nanofibers (CnFs), or graphene nanoplatelets (GnPs) [13]. Conductive coatings applied on both sides of the elongated nitrile rubber glove sections acted as parallel plate electrodes to create a soft capacitor device. The sheet resistance of the conducting and conformal costings was approximately 10 Ω sq^{-1}. The capacitive sensor was attached on the fingertip of a robotic hand to demonstrate force sensing and an accurate force sensing range from 0.03 N to 5 N was achieved during elongation of the curvilinear surfaces. Robinson et al. [14] developed a highly extensible organic capacitive skin comprising of hydrogel electrodes and silicone dielectrics, which were directly 3D printed on soft pneumatic actuators. The use of 3D-printing technology for capacitive sensors enables tactile sensing from external compression and kinesthetic sensing from internal pressurisation. Nur et al. [15] developed highly sensitive capacitive-based strain sensors using an ultrathin wrinkled gold film electrode, which has been used for wearable devices. The strain sensor achieved a gauge factor above 3 and exhibited a high degree of linearity with negligible hysteresis over a maximum applied strain of 140%. Capacitive-type sensors have the potential for soft robotic applications due to their high linearity and low hysteresis; however, a challenge for this technology is the sensors usually have relatively low sensitivity for detecting strain. This is mainly due to the structural properties of the parallel plate capacitors. In addition, it is challenging to manufacture pneumatic self-sensing actuators by directly using the materials that are used for fabricating capacitive sensors.

The integration of resistive, capacitive, and inductive sensing mechanisms can realise multi-functional sensing capability [16–18]. An ultrasensitive multifunctional sensor with two interlocked layers of high-aspect-ratio Pt-coated nanofibers bonded to a flexible substrate was developed by Pang et al. [16]. The sensor can measure and range of mechanical stimuli, including pressure, shear and torsion by using the variation of electrical resistance caused by the change in the conducting path between the two arrays. This multi-functional sensor allowed the intelligent e-skin to be used in a wide range of applications in dynamic signal monitoring in the ultra-low-pressure range. The fabrication process of this form of multi-functional sensing element is relatively complex, and the application is more sensor-based, such as the creation of an e-skin which can be integrated onto the surface of soft actuators, but is challenging to use and to manufacture.

There has therefore been a significant effort to develop flexible piezoresistive sensors for soft robots and wearable devices. A comprehensive review on stretchable and wearable strain sensors and their potential applications has been undertaken in [19]. Piezoresistive materials are often based on electrically conductive fillers, such as carbon-based fillers [20], nanoparticles (NPs) [21,22], wires, or flakes that are embedded in an insulating matrix. Such a composite structure leads to a change in electrical conductivity with stress or strain, as a result of a change in the degree contact between filler particles. Flexible piezoresistive sensors provide the advantages of cost-efficiency, robustness and ease of fabrication [23]. In 2011, Yamada et al. [24] developed a stretchable carbon nanotube strain sensor that could measure strains of up to 280%. When stretched, the nanotube films fracture into isolated islands and bundles that bridge gaps between islands. The formation of these connected islands enables the measurement of strain levels that are 50 times greater than conventional metallic strain gauges. Such carbon nanotube sensors have been embedded into stockings, bandages and gloves to measure

a variety of human motion, including movement, typing, breathing and speech. Yan et al. fabricated a highly stretchable graphene-nanocellulose composite nanopaper for applications that operate at high strain levels of up to 100% [25]. The sensor was implanted in a feather glove to detect the bending and stretching of fingers at strain levels between 35% to 45%. A silver nanowire (AgNW) network and a polydimethylsiloxane (PDMS) elastomer have been used for the fabrication of highly stretchable and sensitive strain sensors [26]. An AgNW thin film was embedded between two layers of PDMS, and the AgNW network-elastomer nanocomposite-based strain sensor exhibited strong piezoresistivity, with tunable gauge factors in the range of 2 to 14 and a high stretchability up to 70%. Liao et al. [27] reported on an effective fabrication strategy to integrate commercial abrasive papers with microcracked gold (Au) nanofilms and developed self-waterproofed crack-based resistive bending strain sensors that could be readily cut to a desired shape. The sensors demonstrated high repeatability, stability and durability of >18,000 strain loading–unloading cycles and a rapid response and relaxation time of 20 ms. The method provides waterproof and robust strain measurement solution for wearable electronic devices and smart health monitoring systems. High-performance flexible strain sensors based on graphene-coated glass fabric/silicone composite were developed by Fu et al. [28]. When compared to conventional flexible strain sensors, the new sensors provide a high strain sensitivity with a gauge factor of approximately 113 and could sustain a high applied force of over 800 N. The sensors showed good piecewise-linear resistance response to both stretching and bending, a high load-bearing capability and a stable response under a cyclic load. Zhang et al. developed an ultrasensitive piezoresistive sensor using silver nanowire (CA) layer-coated polyurethane (PU) sponge. The sensor could measure the motion at a strain range of up to 80%, with a high sensing gauge factor of 26.07 [29]. The sensor displayed exceptional stability, repeatability and durability over 500 cycles. 3D-printing technology has been successfully used for piezoresistive sensor fabrication, Liu et al. presented a fully printed accelerometer with a piezoresistive carbon paste-based strain gauge printed on its surface, which can be manufactured at low cost and with high efficiency. The carbon paste-based strain gauge was fabricated by using screen-printing and direct ink writing technologies, respectively. The sensitivities of the printed accelerometers with the screen-printed strain gauge and direct ink writing strain gauge were 11.99 mV/g and 8.53 mV/g, which have been applied for human motion monitoring [30].

While much of the research has examined attaching or embedding piezoresistive sensors into devices and actuators and developed new materials for manufacturing soft actuators for improved capabilities, such as self-healing [31], less work has aimed at manufacturing soft actuators and robots using the sensing material itself in order to provide robots with an *inherent* sensing capability [32]. Moreover, the current research effort on embedded or integrated sensors predominately uses sensing elements for only direct measurement and signal monitoring. As a result, limited work has been conducted to date on control system design based on the flexible piezoresistive sensors for soft devices or robots. Yang et al. developed pressure and position sensors using piezoresistive elastomers and embedded them into a soft pneumatic finger to mimic human finger motion [33] and to construct an effective closed-loop control system. Koivikko et al. [34] used screen-printed silver conductors as flexible sensors for the measurement and control of soft robotic devices. The sensors were embedded into soft pneumatic fingers to measure the degree of curvature of the actuators. A feedforward control system was constructed to control a three-fingered soft robotic gripper with integrated sensors with a strain up to 2%.

In this paper we use the inherent sensing of an actuator fabricated from a piezoresistive material to achieve a dual feedback control system based on the real-time sensing signals from the soft finger actuator for effective control on the soft finger. The soft actuator is manufactured using a carbon fibre-based piezoresistive composite, which was successfully demonstrated its inherent self-sensing capability during deflation and actuation of a pneumatic soft finger actuator in our previous work [8]. The inherent sensing ability of the soft actuators provides an effective approach to acquiring actuator motion signals without the use of external and embedded sensors. The combination of inherent sensing and dual feedback control can significantly benefit the design of the actuator system, since any

disturbances introduced by the external sensor characteristics and measurement can be eliminated, which could otherwise lead to instability of controller. This new approach, therefore, provides a solution to the current sensing and instrumentation challenges we are facing when design untethered soft actuators or robots.

2. Prototype Development and Characterisation

2.1. Fabrication of Carbon Fibre-Based Flexible Piezoresistive Composite

To create the flexible piezoresistive composite material, short carbon fibres (Easycomposites, mean diameter 7.5 μm, mean length 100 μm) were combined with the individual components of a silicone rubber (E630 silicone rubber; Shenzhen Hong Ye Jie Technology Co., Ltd) and mixed with volume ratio of 0–0.5:1:1 of (carbon fibre)/(part A silicone)/(part B silicone), corresponding to the volume fraction range of 5 vol%, 15 vol% and 20 vol%. The silicone (£8 per kilogram) and short carbon fibres (£27.3 per kilogram) are both cost-efficient materials. The mixture was manually stirred for 10 min to achieve an even distribution of carbon fibres in the silicone. The silicone material has been previously used to create soft actuators and robots due to its low cost and high elastic compliance [35,36]. In order to investigate the versatility of the proposed method, the short carbon fibres used here have twice the mean diameter of the fibres previously used to create piezoresistive composites [8]. The mixture was then subjected to a vacuum atmosphere for 10 min to remove gas, and the carbon fibre/silicone composites were subsequently formed into the required geometry by pouring into a mold of the desired shape and leaving for 24 h at room temperature for the silicone to cure. The shapes formed via the mold were both test samples for electrical and mechanical testing (129 mm × 18 mm × 2.8 mm), as actuator devices. For such a conductive material, a change in electrical resistance with strain is expected due to a change in the degree of carbon fibre filler contact during deformation. Two main challenges have been found in fabricating piezoresistive self-sensing actuators in our research [8]: (i) The addition of a filler should not reduce the compliance of the soft actuator and affect its performance. (ii) The composite must remain conductive and manufacturable to form soft actuators.

2.2. Design and Fabrication of a Self-Sensing Finger Actuator

Using the flexible piezoresistive composite and silicone rubber, a self-sensing soft finger actuator is designed, as shown in Figure 1. The finger consists of two layers; (i) an upper pure silicone teeth layer fabricated using pure silicone to allow maximum mechanical flexibility and deformation and (ii) a lower carbon fibre-rich composite layer fabricated using 15 vol% carbon fibres mixed with silicone to create a piezoresistive layer to provides an inherent sensing capability to the finger. When the finger actuator is pressurised, the upper chambers expand which results in bending of the entire finger, while the lower sensing layer follows the bending and accurately measures finger deformation due to the real-time change of electrical resistance. This new and cost-efficient approach can contribute to addressing current sensing challenge in soft robotics, where embedded or commercial sensors are widely used for real-time strain and pressure measurement.

The fabrication procedure of the self-sensing finger actuator is shown in Figure 2. The molds for casting of a composite finger were manufactured using a commercial 3D printer Ultimaker 2+ using polylactic acid (PLA). 22.8 g carbon fibre (Easycomposites, mean diameter 7.5 μm, mean length 100 μm) and 77.2 g silicone mixture (E630 silicone rubber), corresponding to 15 vol% carbon fibre, were manually stirred for 10 min to achieve an even distribution of carbon fibres in the silicone. The pure silicone was similarly treated and poured into the teeth mold to fabricate the stretchable top layer. The lower sensing layer and upper teeth layer were adhered using silicone adhesive (Smooth-On, Sil-Poxy) and left for 12 h. After completion of the manufacturing process, a silicone tube was then attached to the vent hole of the actuator body using a silicone adhesive (Smooth-On, Sil-Poxy).

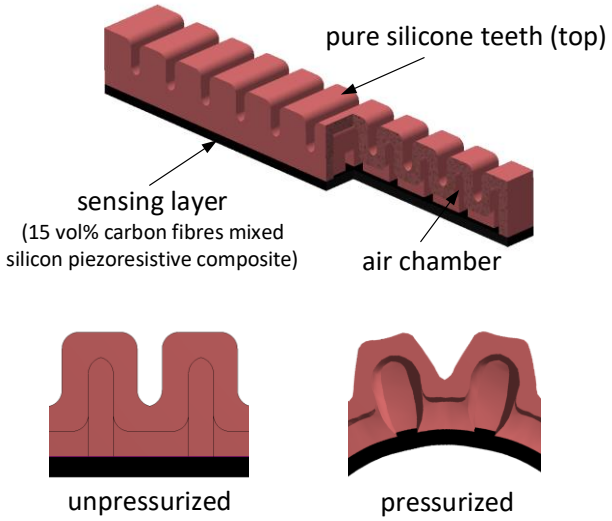

Figure 1. Design of a soft self-sensing finger actuator; the soft finger consists of an upper pure silicone teeth layer and a lower carbon fibre rich composite layer fabricated using 15 vol% carbon fibres mixed with silicone to create the piezoresistive composite.

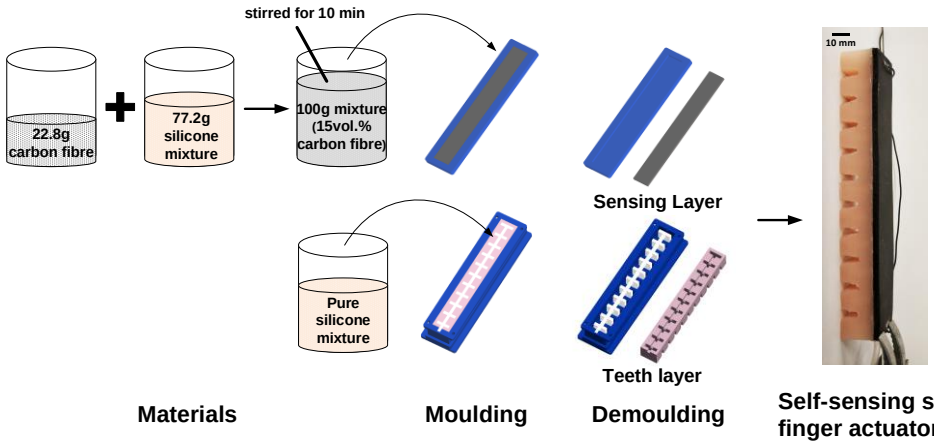

Figure 2. Fabrication of a soft self-sensing finger actuator; finger dimension: 129 mm × 18 mm × 17.5 mm; Carbon sensing layer dimension: 129 mm × 18 mm × 2.8 mm.

2.3. Actuator Sensing Layer Characterisation

Three composite samples with a carbon fibre volume fraction range of 5 vol%, 15 vol% and 20 vol% and a dimension of 129 mm × 18 mm × 2.8 mm were fabricated. The microstructure and distribution of conductive carbon fibres within the insulating silicone matrix were examined using scanning electron microscopy (SEM, JSM6480LV, Tokyo, Japan) on a cryo-fractured sample surface. The SEM image in Figure 3a shows a composite containing 5 vol% carbon fibre, where the carbon fibres are isolated and non-percolated. Such a distribution of conductive fibres leads to electrically insulating properties as there is no contact between the short conductive carbon fibres and thus no electrical circuit is formed through the thickness of the composite. When the volume fraction of carbon fibres increased to 15 vol%, the short carbon fibres begin to make intimate contact with each other and this leads to the creation of electrical short circuits through the thickness of the composite, as shown in Figure 3b. As a result, the composite becomes electrically conductive. For the composite containing carbon fibre at a content of 20 vol% in Figure 3c, there is a high degree of filler contact and percolation, which results in the material behaving as a highly sensitive conductor. These findings agree with our previous study in Ref. [8] that used smaller diameter fibres (mean diameter 3.55 μm and mean length 105 μm), and it can be concluded that the mean diameter of the carbon fibres does not significantly

affect the degree of filler percolation and the conductivity of the composite, which demonstrates the versatility of the proposed approach. In this work, a piezoresistive composite with 15 vol% carbon fibres mixed with silicone was used to manufacture the actuator due to its low viscosity for molding and good piezoresistive response for sensing.

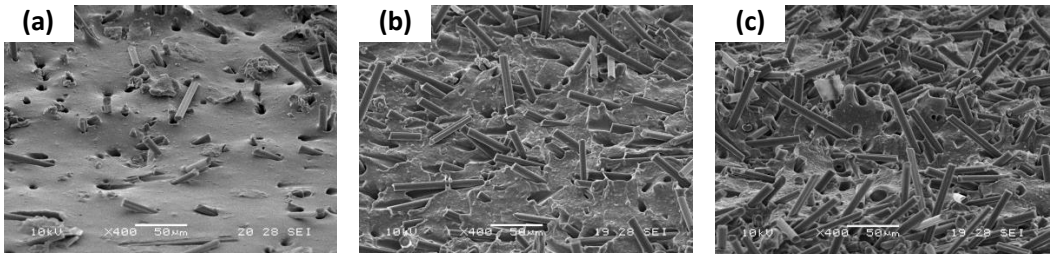

Figure 3. Cryo-fracture surface carbon fibre/silicone composites containing carbon fibre. (**a**) 5 vol%, (**b**) 15 vol% and (**c**) 20 vol%.

To examine the piezoresistive properties of the sensing layer and test its performance as a strain sensor, the frequency-dependent electrical properties (AC conductance amplitude and phase) as a function of strain was characterised. This was achieved by electrical measurement of the sensing region while being subjected to a tensile strain in a Hounsfield mechanical test machine. The sample was placed in the test machine with two electrodes with a distance of 47 mm attached to the surface of the sample. Two pneumatic clamps at a 100 mm separation with a small tensile load were used to locate the sample. The sample was stretched to deformation levels from 0 to 10 mm, with a step size of 1 mm.

The short carbon fibre–silicone composite can be considered and as a random resistor–capacitor (*R*–*C*) network, where the resistors (*R*) in the network represents the conductive carbon fibres which have a frequency-independent admittance ($Y_{ac} = 1/Z$, where Z is the impedance) and the capacitor (*C*) represents the electrically insulating and capacitive silicone matrix with a frequency-dependent admittance ($Y_{ac} \propto \omega C$). At low frequencies, any AC current will flow preferentially through the percolated carbon fibres since $R^{-1} > \omega C$ with a corresponding phase angle that approaches 0° since both current and voltage are in phase for a resistor, see Figure 4. As the sensing layer is deformed and aligned in the direction of strain, the thickness of the composite will decrease, and the carbon fibres will make better contact in the thickness direction, which result in an increase in its admittance. At high frequencies the AC conductivity of the capacitive regions increases and when $\omega C \geq R^{-1}$, the capacitive silicone regions also contribute to the AC currents so that the phase angle decreases with increasing frequency and begins to approach −90°. As a result, it is important to undertake electrical measurements at a sufficiently low frequency for the successful implementation of the sensing layer.

Figure 4 shows that the composites with 15 vol% of carbon fibre is behaving as a conductor, with a frequency-independent admittance (Figure 4a), with a corresponding phase angle of 0° at deformation levels up to 10 mm below frequencies of 100 Hz (Figure 4b). At frequencies higher than 100 Hz the phase angle begins to decrease as a result of an increase in the capacitive contribution (ωC) to the overall conductivity, although this effect remains small.

The strain and resistance relationship can be derived from the AC admittance testing results, as shown in Figure 5, where the relative resistance ($R = 1/G$) is obtained at a fixed frequency of 1 Hz. This calibrated relationship can be used to measure the deformation strain of the soft actuator using the change of resistance.

Figure 6 shows the cyclic variation of resistance and the force–displacement response of the soft finger sensing layer with a dimension of 129 mm × 18 mm × 2.8 mm. The sensing layer was subjected to a cyclic strain using an Instron 3369 with a 50 N static load cell and pneumatic clamps with a small tensile load and a cyclic deformation of 2 mm at a crosshead speed of 2 mm/min. The distance between the electrodes for the measurement was 78 mm. A degree of hysteresis is observed, which is typical of an elastomer material, and the effect could be compensated by using feedback control approach

when calibrating the sensors. The force–displacement of the composite leads to a cyclical change in resistance of the composite.

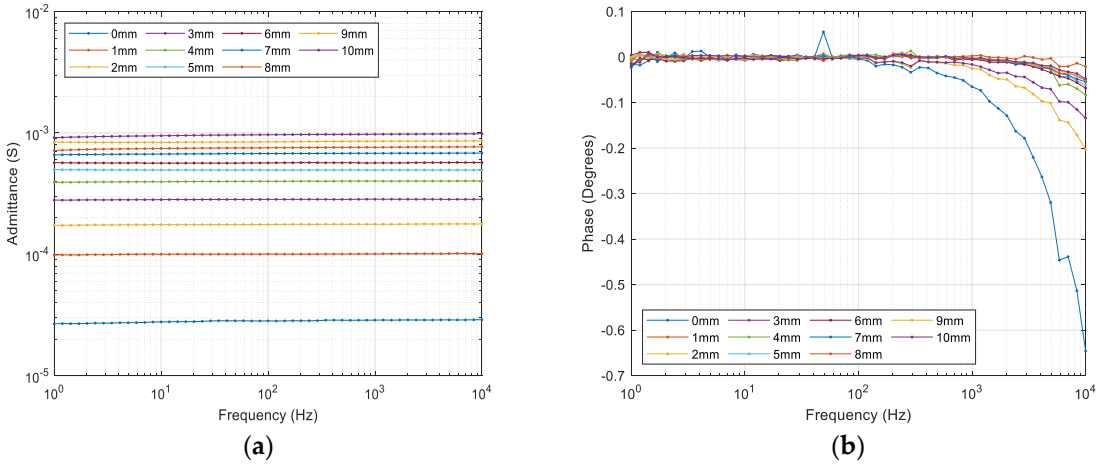

Figure 4. (**a**) Variation in AC admittance with extension for carbon fibre/silicone composites containing 15 vol% carbon fibre. (**b**) Variation in phase angle with extension for carbon fibre/silicone rubber composites containing 15 vol% carbon fibre.

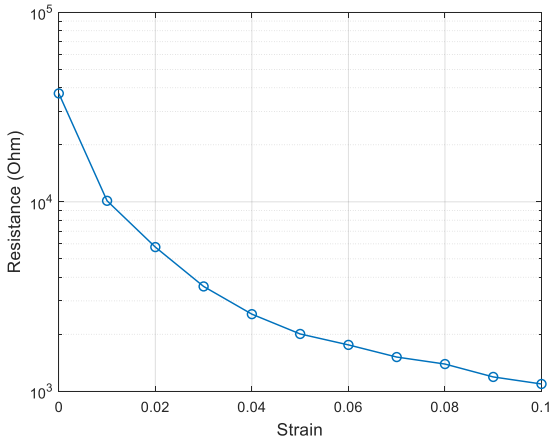

Figure 5. Strain and resistance (at 1 Hz) relationship achieved from AC admittance test.

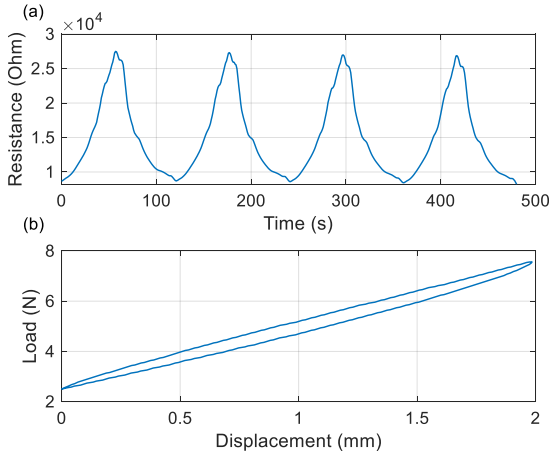

Figure 6. Cyclic response of (**a**) resistance–time (**b**) load force–displacement during cyclic testing of the sensing bottom layer.

3. Controllable Self-Sensing Soft Finger Actuator

3.1. Real-time Sensing Measurement

The soft self-sensing finger was actuated by an air compressor (9.6 CFM, 0–10 bar, Wolf Sioux) and the actuation pressure was measured by a pressure gauge (CYYZ11, Star Sensors). The experimental setting-up of the self-sensing finger actuator is shown in Figure 7a and the time-lapse images from the high-speed video is shown in Figure 7b. A high-speed camera, Photron FASTCAM Mini UX100 was used to capture the motion of the soft finger. The camera was placed on a tripod in front of the soft finger at approximately 1 m distance to enable a sufficient view of the whole soft finger when inflated at its maximum pressure. The driven pressure is controlled by the pressure regulator of the air compressor and gradually increasing from 0 bar to the maximum pressure of 2.1 bar, corresponding to the maximum bending degree of 144.27°. The distance between the electrodes for characterisation of electrical resistance is 123 mm.

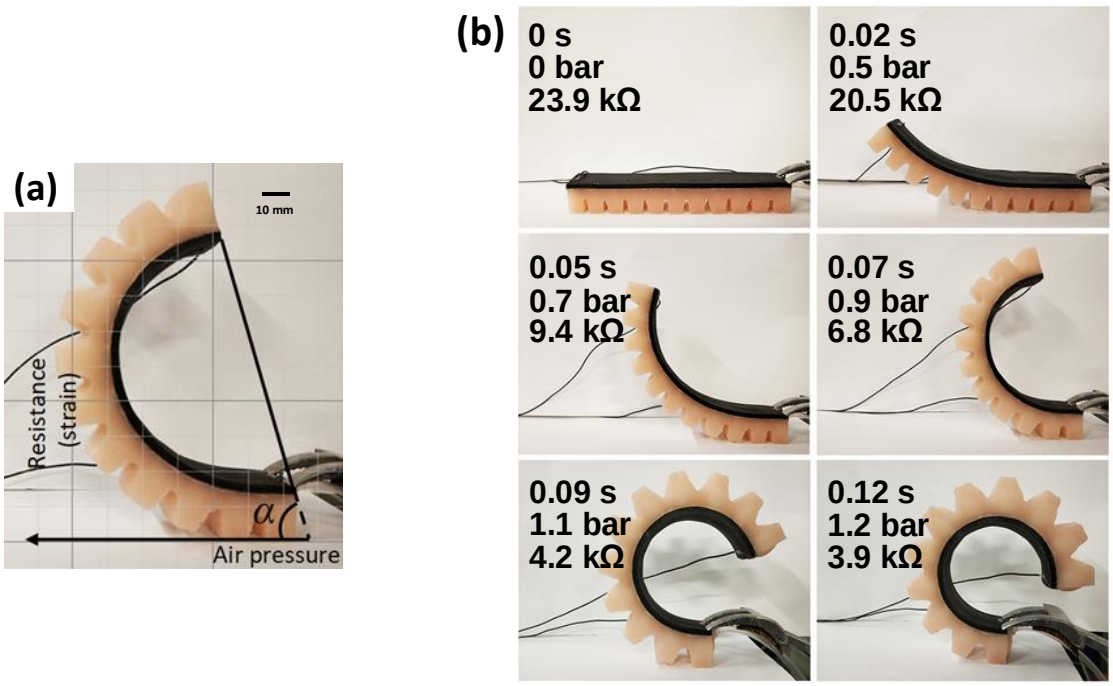

Figure 7. (**a**) Experimental set-up of self-sensing finger actuator. (**b**) Time-lapse images from high-speed video of the self-sensing finger actuator showing time, pressure and inherent resistance.

The measured resistance against a real-time driven pressure that was increasing from 0 bar to 1.2 bar is shown in Figure 8a, where the strain can be obtained through the calibrated resistance–strain relationship in Figures 5 and 8b. This enables real-time measurement of the deformation of the finger, which can be used for the construction of a feedback control system. Note that the first cycle of operation tends to show an altered response due to a relaxation phenomenon and thus an initialisation cycle is required before this deformation measurement can be obtained. An approximated linear relationship between the strain and pressure is obtained, which shows the self-sensing actuator functions effectively as a strain sensor during its inflation and deflation. A degree of hysteresis was observed when the finger was pressurised and depressurised, see Figure 8a. Potential reasons can be (i) changes in the distribution of the carbon fibres, or levels of contact, after being subjected to large deformations or (ii) the hysteretic nature of the silicone matrix.

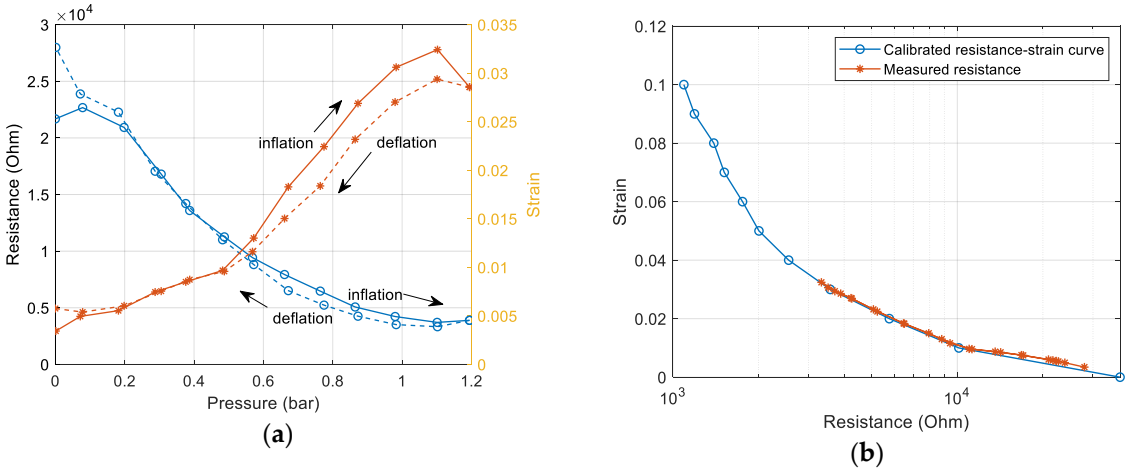

Figure 8. (**a**) Measured real-time resistance and strain against the driven pressure from 0 to 1.2 bar. (**b**) Calibrated resistance–strain relationship (Figure 5) and measured resistance from the self-sensing finger (Figure 8a).

Figure 8a shows the relationship between the driven pressure and bending angle $\alpha$of the soft finger. The highest pressure difference between the inflation and deflation occurred at a bending angle of approximately 80° and indicates that some degree of strain hysteresis originates from the silicone material. Using the relationship of pressure and strain in Figure 8a and the results from Figure 9a, the relationship of the bending angle α and strain can be derived, as shown in Figure 9b, where an approximated linear equation can be achieved. The sensing layers have potential for accurate sensing in a range of soft applications, where the sensitivity is 24 kΩ in the strain range of 4–10% and 870 kΩ in the strain range of 0–4%.

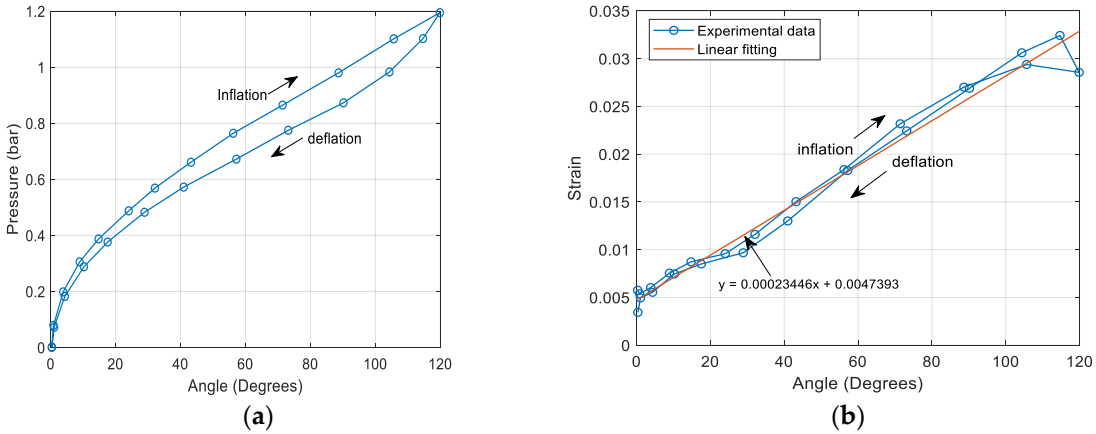

Figure 9. (**a**) Measured real-time bending angle against the driven pressure from 0 to 1.2 bar. (**b**) Angle–strain relationship and its linear approximation.

3.2. Control System for a Self-Sensing Finger Actuator

To effectively control the soft finger and obtain the desired positions, a closed-loop control system with PI (proportional-integral) feedback is designed in MATLAB Simulink 2019a. Figure 10 shows a schematic of the dual-loop control system, which consists of a position and pressure control section. The position controller generates the desired pressure using the error of the bending angle. An angle filter is used to convert the sensory output from a strain to an angle, see Figure 9b. The measured pressure is fed into the pressure controller to generate the desired driving voltage for the soft finger to obtain the desired position. The angle–pressure model is constructed based on the relationship in Figure 9a using a mapping block, and a valve calibration model is created from the characteristics

of the pneumatic proportional directional control valve (Festo MPYE-5-M5-010-B), which is used to control the soft finger. These blocks are used as a command feedforward to increase the speed of response in comparison to the PI controllers alone.

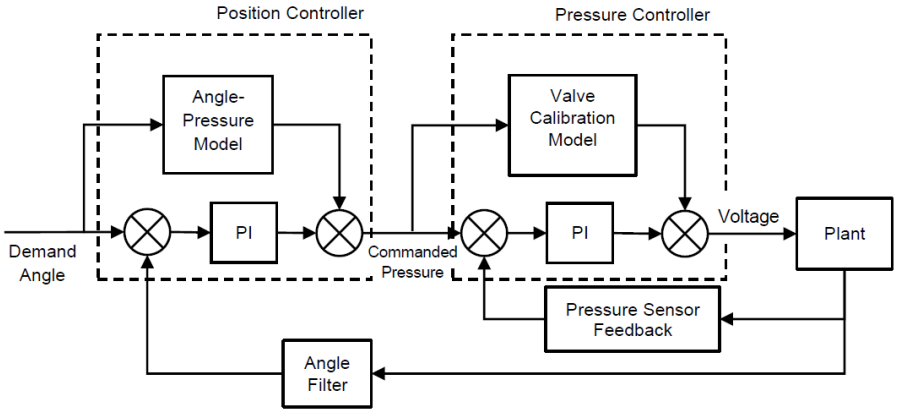

Figure 10. Block diagram of the designed closed-loop controller.

Figure 11 shows the simulation results of the actual and desired positions of the soft finger when it was driven by step inputs. The step inputs from 0° to 45° and 0° to 90° were used to investigate the system dynamic responses and the measured rise times are 1.1 s and 2.2 s, respectively, without an overshoot. The rise time is defined as the time taken for a response to rise from 10% to 90% of its steady-state value. These results show that the designed control system is effective and robust to the sudden change of the system. For the pressure controller, the gain P_p and I_p are tuned as 5.0 and 1.0; while for the position controller, the gain P_θ and I_θ are tuned to 0.05 and 0.04.

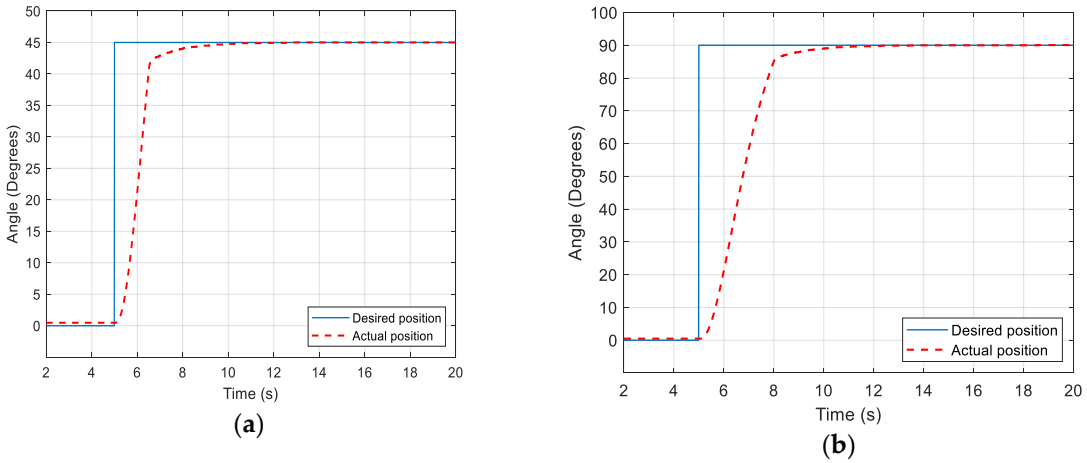

Figure 11. Simulated actual and desired positions of the soft finger with a step driven input. (**a**) The step input from 0° to 45°. (**b**) The step input from 0° to 90°.

Figure 12 shows the simulated actual and desired angles of the soft finger when the pulse signals were applied as a demand, and the period of the pulse signal is 20 s. The pulse input was set from 20° to 45°, and an overshoot was observed during the retraction, with a value of 3.0° and a percentage of 12%. The rise time is approximately 0.4 s during the inflation stage and 1.2 s during the deflation stage. Increasing the pulse boundary to 90°, the overshoot during the retraction is approximately 2.5°, as shown in Figure 12b. The rise time is about 1.3 s during inflation and 2.0 s during deflation. The results show that the designed controller can effectively control the finger motion, and the control system is robust to the sudden changes in angle position.

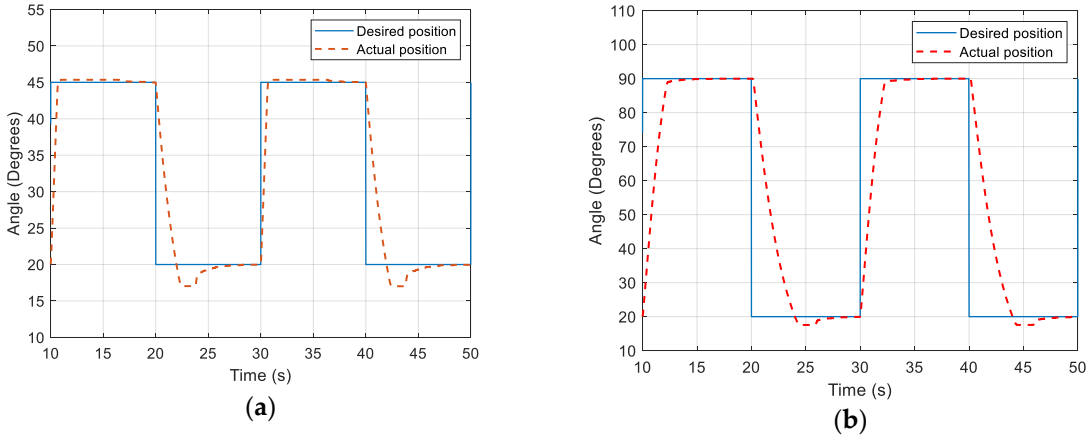

Figure 12. Simulated actual and desired positions of the soft finger with a pulse driven input (pulse period = 20 s). (**a**) The pulse input from 20° to 45°. (**b**) The pulse input from 20° to 90°.

Simulated results show that the designed control system is effective to control the self-sensing finger actuator using a feedback control configuration. This demonstrates the feasibility of manufacturing and using a self-sensing actuator as a sensor for the development of a control system, which contributes to the development of a soft controllable self-sensing actuator. Further investigation will consider increasing the accuracy and robustness of the self-sensing measurement and reducing resistance drift during measurement. However, this could be overcome if the change of the resistance ΔR is consistent, which could be employed in the control system instead of using the absolute resistance measurement R directly.

4. Conclusions

Carbon fibre-based piezoresistive composites were created and used to successfully manufacture a self-sensing layer of a pneumatic soft finger actuator, where the change in resistance of the actuator body was used to monitor deformation with applied pressure and finger motion control. The sensing materials can be used to manufacture an integrated sensing finger, in which the whole body has an inherent sensing capability. The advantage of the complete actuator being fabricated from such a piezoresistive composite is that multiple electrodes could be used to understand soft actuator deformation in a range of directions and thus perform effective control strategies for desired motion.

The inherent self-sensing functionality can significantly benefit the design of control systems, since any undesirable disturbances introduced by the presence of an external or embedded sensor, which can cause instability of controller, can be effectively eliminated. As an example, the use of and inherent piezoresistive sensing layer does not influence the flexibility of the actuator for deformations with a strain up to 10%. The results show that the strain sensing layer is sufficient to measure large deformation of the actuator and the newly designed dual-closed-loop feedback controller is a promising approach to conduct position control. Continuous real-time experiments will be carried out to validate the reliability of the controller and the consistency of the measurement achieved from the soft finger. We have observed a maximum of 10° angle difference between the piezoresistive sensing measurement and the camera-tracked image when used an open-loop controller. A reliability study will be conducted to investigate the sensing error tolerance of self-sensing actuator.

Our new approach provided a promising solution for mass manufacturing, accurate modelling and control of soft actuators and robots, including the creation of new composites, fabrication, modelling and control of the self-sensing finger. The force and bandwidth of the actuator are highly dependent on the drive mechanism. In this work, the self-sensing actuator is pneumatically driven, which has a relatively low bandwidth of approximately 5 Hz. The maximum operating pressure was 2 bar in our experiments and the actuator characteristics are repeatable. The addition of carbon fibre fillers does not reduce the compliance of the soft actuator and affect its static and dynamic performance,

which is a significant advantage of this new approach. Potential future research directions are the use of multiple electrodes to provide information of multi-axial deformation and ultimately determine actuator shape, and the use of multifunctional composites to create soft actuators or robots capable of sensing additional parameters such as pressure, displacement, speed, temperature, magnetic fields and moisture.

Author Contributions: Conceptualisation and methodology, M.P. and C.B.; experimental validation, H.A., C.Y.; control system design and analysis, H.A., A.P.; data analysis, M.P., J.Z. (Jun Zou), J.Z. (Junhui Zhang); writing—original draft preparation, M.P.; writing—review and editing, M.P., C.B., A.P., J.Z. (Jun Zou), and J.Z. (Junhui Zhang). All authors have read and agreed to the published version of the manuscript.

Funding: This work was supported in part by the Royal Society Research Grant (RGS\R2\180110), the University of Bath Alumni Fund (F1920A-RS02), the Open Foundation of the State Key Laboratory of Fluid Power and Mechatronic Systems, Zhejiang University, China, grant number GZKF-201801 and the China Scholarship Council PhD studentship (201706150102).

Acknowledgments: We thank Stephen Coombes for contributing to the wiring and electrodes of the sensing layer of the soft finger actuator.

Conflicts of Interest: The authors declare no conflict of interest.

References

1. Cianchetti, M.; Laschi, C.; Menciassi, A.; Dario, P. Biomedical applications of soft robotics. *Nat. Rev. Mater.* **2018**, *3*, 143–153. [CrossRef]
2. Ranzani, T.; Gerboni, G.; Cianchetti, M.; Menciassi, A. A bioinspired soft manipulator for minimally invasive surgery. *Bioinspir. Biomim.* **2015**, *10*, 035008. [CrossRef]
3. Oguntosin, V.; Harwin, W.S.; Kawamura, S.; Nasuto, S.J.; Hayashi, Y. Development of a wearable assistive soft robotic device for elbow rehabilitation. In Proceedings of the 2015 IEEE International Conference on Rehabilitation Robotics (ICORR), Singapore, 11–14 August 2015; pp. 747–752.
4. Kim, J.; Lee, G.; Heimgartner, R.; Revi, D.A.; Karavas, N.; Nathanson, D.; Galiana, I.; Eckert-Erdheim, A.; Murphy, P.; Perry, D.; et al. Reducing the metabolic rate of walking and running with a versatile, portable exosuit. *Science* **2019**, *365*, 668–672. [CrossRef] [PubMed]
5. Manti, M.; Pratesi, A.; Falotico, E.; Cianchetti, M.; Laschi, C. Soft assistive robot for personal care of elderly people. In Proceedings of the 2016 6th IEEE International Conference on Biomedical Robotics and Biomechatronics (BioRob), Singapore, 26–29 June 2016; pp. 833–838.
6. Katzschmann, R.K.; DelPreto, J.; MacCurdy, R.B.; Rus, D. Exploration of underwater life with an acoustically controlled soft robotic fish. *Sci. Robot.* **2018**, *3*, eaar3449. [CrossRef]
7. Miriyev, A.; Stack, K.; Lipson, H. Soft material for soft actuators. *Nat. Commun.* **2017**, *8*, 596. [CrossRef] [PubMed]
8. Yan, X.; Bowen, C.R.; Yuan, C.; Hao, Z.; Pan, M. Carbon fibre based flexible piezoresistive composites to empower inherent sensing capabilities for soft actuators. *Soft Matter* **2019**, *15*, 8001–8011. [CrossRef] [PubMed]
9. Roberts, P.; Damian, D.D.; Shan, W.; Lu, T.; Majidi, C. Soft-matter capacitive sensor for measuring shear and pressure deformation. In Proceedings of the 2013 IEEE International Conference on Robotics and Automation, Karlsruhe, Germany, 6–10 May 2013; pp. 3529–3534.
10. Shapiro, Y.; Kosa, G.; Wolf, A. Shape Tracking of Planar Hyper-Flexible Beams via Embedded PVDF Deflection Sensors. *IEEE/ASME Trans. Mechatron.* **2013**, *19*, 1260–1267. [CrossRef]
11. Yang, H.; Qi, D.; Liu, Z.; Chandran, B.K.; Wang, T.; Yu, J.; Chen, X. Soft thermal sensor with mechanical adaptability. *Adv. Mater.* **2016**, *28*, 9175–9181. [CrossRef]
12. Hammock, M.L.; Chortos, A.; Tee, B.C.K.; Tok, J.B.-H.; Bao, Z. 25th Anniversary Article: The Evolution of Electronic Skin (E-Skin): A Brief History, Design Consideration s, and Recent Progress. *Adv. Mater.* **2013**, *25*, 5997–6038. [CrossRef]
13. Cataldi, P.; Dussoni, S.; Ceseracciu, L.; Maggiali, M.; Natale, L.; Metta, G.; Athanassiou, A.; Bayer, I.S. Carbon Nanofiber versus Graphene-Based Stretchable Capacitive Touch Sensors for Artificial Electronic Skin. *Adv. Sci.* **2017**, *5*, 1700587. [CrossRef]

14. Robinson, S.S.; O'Brien, K.W.; Zhao, H.; Peele, B.N.; Larson, C.M.; Mac Murray, B.; Van Meerbeek, I.M.; Dunham, S.N.; Shepherd, R.F. Integrated soft sensors and elastomeric actuators for tactile machines with kinesthetic sense. *Extreme Mech. Lett.* **2015**, *5*, 47–53. [CrossRef]
15. Nur, R.; Matsuhisa, N.; Jiang, Z.; Nayeem, O.G.; Yokota, T.; Someya, T. A Highly Sensitive Capacitive-type Strain Sensor Using Wrinkled Ultrathin Gold Films. *Nano Lett.* **2018**, *18*, 5610–5617. [CrossRef] [PubMed]
16. Pang, C.; Lee, G.-Y.; Kim, T.-I.; Kim, S.M.; Kim, H.N.; Ahn, S.-H.; Suh, K.-Y. A flexible and highly sensitive strain-gauge sensor using reversible interlocking of nanofibres. *Nat. Mater.* **2012**, *11*, 795–801. [CrossRef] [PubMed]
17. Guo, J.-L.; Rossiter, J. Stretchable bifilar coils for soft adhesion and sensing. *Mater. Des.* **2020**, *190*, 108545. [CrossRef]
18. Din, S.; Xu, W.; Cheng, L.K.; Dirven, S. A Stretchable Multimodal Sensor for Soft Robotic Applications. *IEEE Sens. J.* **2017**, *17*, 5678–5686. [CrossRef]
19. Amjadi, M.; Kyung, K.-U.; Park, I.; Sitti, M. Stretchable, Skin-Mountable, and Wearable Strain Sensors and Their Potential Applications: A Review. *Adv. Funct. Mater.* **2016**, *26*, 1678–1698. [CrossRef]
20. Zhang, W.; Dehghani-Sanij, A.A.; Blackburn, R.S. Carbon based conductive polymer composites. *J. Mater. Sci.* **2007**, *42*, 3408–3418. [CrossRef]
21. Wang, S.; Zhang, X.; Wu, X.; Lu, C. Tailoring percolating conductive networks of natural rubber composites for flexible strain sensors via a cellulose nanocrystal templated assembly. *Soft Matter* **2016**, *12*, 845–852. [CrossRef]
22. Khalili, N.; Shen, X.; Naguib, H.E. An interlocked flexible piezoresistive sensor with 3D micropyramidal structures for electronic skin applications. *Soft Matter* **2018**, *14*, 6912–6920. [CrossRef]
23. Zhao, S.; Li, J.; Cao, D.; Zhang, G.; Li, J.; Li, K.; Yang, Y.; Wang, W.; Jin, Y.; Sun, R.; et al. Recent Advancements in Flexible and Stretchable Electrodes for Electromechanical Sensors: Strategies, Materials, and Features. *ACS Appl. Mater. Interfaces* **2017**, *9*, 12147–12164. [CrossRef]
24. Yamada, T.; Hayamizu, Y.; Yamamoto, Y.; Yomogida, Y.; Izadi-Najafabadi, A.; Futaba, D.N.; Hata, K. A stretchable carbon nanotube strain sensor for human-motion detection. *Nat. Nanotechnol.* **2011**, *6*, 296–301. [CrossRef] [PubMed]
25. Yan, C.; Wang, J.; Kang, W.; Cui, M.; Wang, X.; Foo, C.Y.; Chee, K.J.; Lee, P.S. Highly Stretchable Piezoresistive Graphene-Nanocellulose Nanopaper for Strain Sensors. *Adv. Mater.* **2013**, *26*, 2022–2027. [CrossRef] [PubMed]
26. Amjadi, M.; Pichitpajongkit, A.; Lee, S.; Ryu, S.; Park, I. Highly Stretchable and Sensitive Strain Sensor Based on Silver Nanowire–Elastomer Nanocomposite. *ACS Nano* **2014**, *8*, 5154–5163. [CrossRef] [PubMed]
27. Liao, X.; Zhang, Z.; Liang, Q.; Liao, Q.; Liao, X. Flexible, Cuttable, and Self-Waterproof Bending Strain Sensors Using Microcracked Gold Nanofilms@Paper Substrate. *ACS Appl. Mater. Interfaces* **2017**, *9*, 4151–4158. [CrossRef]
28. Fu, Y.-F.; Li, Y.-Q.; Liu, Y.-F.; Huang, P.; Hu, N.; Fu, S.-Y. High-Performance Structural Flexible Strain Sensors Based on Graphene-Coated Glass Fabric/Silicone Composite. *ACS Appl. Mater. Interfaces* **2018**, *10*, 35503–35509. [CrossRef]
29. Zhang, S.; Liu, H.; Yang, S.; Shi, X.; Zhang, D.; Shan, C.; Mi, L.; Liu, C.; Shen, C.; Guo, Z. Ultrasensitive and Highly Compressible Piezoresistive Sensor Based on Polyurethane Sponge Coated with a Cracked Cellulose Nanofibril/Silver Nanowire Layer. *ACS Appl. Mater. Interfaces* **2019**, *11*, 10922–10932. [CrossRef]
30. Liu, M.; Zhang, Q.; Zhao, Y.-L.; Shao, Y.; Zhang, D. Design and Development of a Fully Printed Accelerometer with a Carbon Paste-Based Strain Gauge. *Sensors* **2020**, *20*, 3395. [CrossRef]
31. Terryn, S.; Roels, E.; Brancart, J.; Van Assche, G.; VanderBorght, B. Self-Healing and High Interfacial Strength in Multi-Material Soft Pneumatic Robots via Reversible Diels–Alder Bonds. *Actuators* **2020**, *9*, 34. [CrossRef]
32. Walker, J.; Zidek, T.; Harbel, C.; Yoon, S.; Strickland, F.S.; Kumar, S.; Shin, M. Soft Robotics: A Review of Recent Developments of Pneumatic Soft Actuators. *Actuators* **2020**, *9*, 3. [CrossRef]
33. Yang, Y.; Chen, Y. Innovative Design of Embedded Pressure and Position Sensors for Soft Actuators. *IEEE Robot. Autom. Lett.* **2017**, *3*, 656–663. [CrossRef]
34. Koivikko, A.; Raei, E.S.; Mosallaei, M.; Mantysalo, M.; Sariola, V. Screen-Printed Curvature Sensors for Soft Robots. *IEEE Sens. J.* **2018**, *18*, 223–230. [CrossRef]

35. Jiao, Z.; Ji, C.; Zou, J.; Yang, H.; Pan, M. Vacuum-Powered Soft Pneumatic Twisting Actuators to Empower New Capabilities for Soft Robots. *Adv. Mater. Technol.* **2018**, *4*, 1800429. [CrossRef]
36. Jiao, Z.; Zhang, C.; Wang, W.; Pan, M.; Yang, H.; Zou, J. Advanced Artificial Muscle for Flexible Material-Based Reconfigurable Soft Robots. *Adv. Sci.* **2019**, *6*. [CrossRef] [PubMed]

© 2020 by the authors. Licensee MDPI, Basel, Switzerland. This article is an open access article distributed under the terms and conditions of the Creative Commons Attribution (CC BY) license (http://creativecommons.org/licenses/by/4.0/).